Monte Carlo calculations of photon spectra in air from 192Ir sources

Borg, J.; Rogers, D. W. O.

https://doi.org/10.4224/5764262

Monte Carlo Calculations of Photon Spectra in Air from ^{192}Ir Sources

J. Borg and D. W. O. Rogers

March, 1999

PIRS-629r

Ionizing Radiation Standards
Institute for National Measurement Standards
National Research Council
Ottawa, Ontario, K1A 0R6, Canada

Telephone: (613) 993-2715
Fax: (613) 952-9865
E-mail: dave@irs.phy.nrc.ca

ABSTRACT

We determine the spectra of the primary and scattered photons around different types of ^{192}Ir sources used in HDR brachytherapy. The air-kerma strength per unit activity is calculated for these sources at distances ranging from the surface of the source to 50 cm in air and in vacuum. The effect of bin-size for scoring the fluence spectrum is studied to avoid binning artefacts and to use an acceptable amount of memory. A bin-size of 5 keV is found to be adequate for ^{192}Ir. The calculated air-kerma strength for four sources, *i.e.* the microSelectron HDR source, the VariSource and the seed sources from Best Industries, Inc., and Alpha-Omega Services, Inc., agree well with previous results by other authors considering the differences, *e.g.* spectral data and mass energy-absorption coefficients, between the calculations. The air-kerma strength for the bare source is $2-12\%$ higher than for the encapsulated sources due to the attenuation and absorption in the core and the encapsulating material, when photons with energy less than 60 keV are not taken into account. For the full spectrum this difference is up to 23% due to the large air-kerma contribution from the unfiltered low-energy photons. The contribution to the air-kerma strength from scattered photons and from bremsstrahlung are calculated for the four types of encapsulated sources and increase the air-kerma strength by $2-4\%$ and $0.2-0.3\%$, respectively.

This is the revised version of PIRS-629. The difference is the inclusion of the VariSource.

Contents

1. Introduction

EGS4 Monte Carlo calculations of the photon spectra from different types of ^{192}Ir seed sources were performed by C. Thomason *et al.*[1,2] in 1989. D. Rogers made similar Monte Carlo calculations in Oct. 1992 to verify the spectra and in particular to study the generation of photons with energy below 10 keV, which were present in the spectra calculated by Thomason.[1] Rogers' calculations did not verify the contribution from the low-energy photons (< 10 keV), and further studies were required. In 1994, Büermann *et al.*[3] reported the air-kerma rate constants for the microSelectron-HDR (High Dose Rate) source and the ^{192}Ir point source.

In this report, a similar Monte Carlo calculation is performed with the latest spectral data for the ^{192}Ir nuclide and values of the mass energy-absorption coefficients in air. The fluence spectrum around four types of ^{192}Ir sources and for a bare ^{192}Ir point source is calculated using the FLURZ EGS4 user-code. The air-kerma strength per unit source activity is calculated at several distances from the cylinder axis, *i.e.* on surface, at 1, 2, 5, 10, 20 and 50 cm distance.

The purpose of this work is to obtain energy spectra around the ^{192}Ir sources for use in future Monte Carlo simulations of ionization-chamber experiments, and to evaluate the influence of the different geometries and the different encapsulating materials of the sources.

1.1. History

The work on standardization of the radionuclide ^{192}Ir was begun in early 1977 by the National Bureau of Standards (NBS)[4] in collaboration with the companies supplying the sources. In 1988, the American Association of Physicists in Medicine (AAPM) formed Task Group No. 43. They were to recommend a dosimetry protocol including a formalism for dose calculations and a data set for the values of dosimetry parameters.[5] A historical review of dosimetry calculations and measurements for interstitial brachytherapy sources from 1966 to 1991 is given by Nath *et al.*[5] in The Report of TG-43.

Previously, the exposure-rate constant, Γ_δ, relating the exposure rate to the source activity was used. In the new terminology this quantity corresponds to the air-kerma strength per unit source activity, S_k/A, where the air-kerma strength is a measure of brachytherapy source strength. The exposure-rate constant and the air-kerma strength are defined in Section 1.2.1. Using the air-kerma strength - a quantity to be measured - to specify the source strength is better than using the source activity multiplied by the exposure rate constant, since the latter depend on how well the manufacturer can specify the activity.

1.2. Air-kerma strength

1.2.1. Definitions

Air-kerma strength is a measure of brachytherapy source strength, which is specified in terms of air-kerma rate at a point along the transverse axis of the source in free space.[5] It is defined as the product of air-kerma rate at a calibration distance, d, in free space, $\dot{K}_{air}(d)$, measured along the transverse bisector of the source, and the square of the distance, d:

$$S_k = \dot{K}_{air}(d) \cdot d^2 \qquad [\mu\text{Gy m}^2\ \text{h}^{-1}] \tag{1}$$

The calibration distance must be large enough that the source may be treated as a mathematical point. In practice, the air-kerma rate standardization measurements are performed in air and corrections for air attenuation are applied if needed. Since the measurements for source-strength calibration may be performed at any large distance, d, the air-kerma rate is normally specified in terms of a reference calibration distance, d_0, which is usually chosen to be 1 m.

The unit of S_k is denoted by the symbol U:[5]

$$1\ \text{U} = 1\ \ \mu\text{Gy m}^2\ \text{h}^{-1} \tag{2}$$

The previously used quantity the exposure-rate constant, Γ_δ, of a radioactive nuclide emitting photons is the quotient of $l^2(dX/dt)_\delta$ by A, where $(dX/dt)_\delta$ is the exposure rate due to photons of energy greater than δ, at a distance, l, from a point source of this nuclide having activity A:[6]

$$\Gamma_\delta = (dX/dt)_\delta \cdot \frac{l^2}{A} \qquad [\text{R cm}^2\ \text{mCi}^{-1}\ \text{h}^{-1}] \tag{3}$$

1.2.2. From exposure-rate constant to air-kerma strength

The collision kerma in dry air, $(K_c)_{air}$, is calculated from the exposure, X:

$$(K_c)_{air}\ \ [\text{J kg}^{-1}] = X\ \ [\text{C kg}^{-1}] \cdot \left(\frac{\bar{W}}{e}\right)_{air}\ \ [\text{J C}^{-1}]\ , \tag{4}$$

where $\bar{W}$ is the average energy required to produce an ion pair in dry air, and e is the elementary charge. $(\bar{W}/e)_{air} = 33.97$ J C^{-1}. The conversion from [R] to [C kg^{-1}] is:[7]

$$X\ \ [\text{R}] = 2.580 \cdot 10^{-4}\ X\ \ [\text{C kg}^{-1}] \tag{5}$$

The relation between exposure-rate constant in [R cm^2 mCi^{-1} h^{-1}] and air-kerma strength per unit activity in [μGy m^2 Bq^{-1} h^{-1}] is then:

$$1\ \ \text{R cm}^2\ \text{mCi}^{-1}\ \text{h}^{-1} = 2.369 \cdot 10^{-8}\ \ \text{U Bq}^{-1} \tag{6}$$

1.3. Bare ^{192}Ir spectra

Over the years, bare ^{192}Ir spectra have been presented, *e.g.* by Glasgow and Dillman (1979),[8] by Kocher (1981),[9] by NCRP (1985),[10] and by Duchemin and Coursol (1993).[11] There are only slight changes in these data, and the most recent data we are aware of, have been used in this work, *i.e.* the data published in a technical note from DAMRI, CEA, France, in 1993.

^{192}Ir decays through 4.7% electron capture and 95.3% β^- transitions, followed by γ transitions and K- and L-shell x-rays. The energy distribution of the initial photons from the ^{192}Ir radionuclide is shown in Fig. 1 (see also Appendix A1).

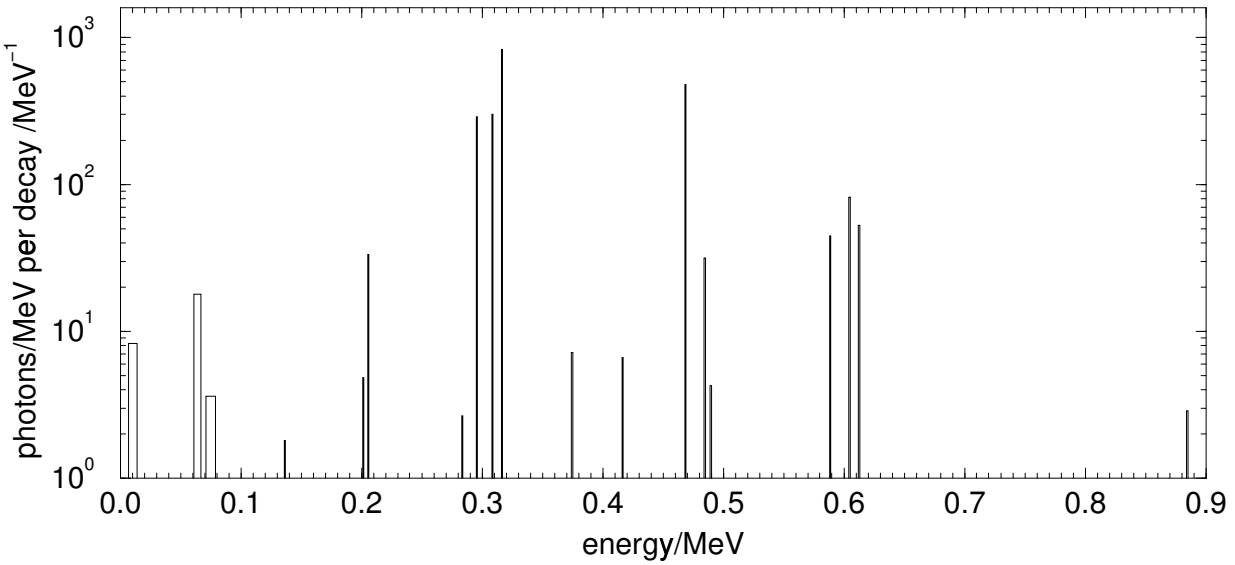

Figure 1: Photon spectrum for ^{192}Ir radionuclide used as input spectrum for the Monte Carlo calculations. The number of photons are divided by the bin width, which is 6-8 keV for the three lower bins and 1 keV for the rest. The data are from Duchemin and Coursol, 1993.[11] Values are tabulated in Appendix A1.

The half-life for ^{192}Ir is 73.825 days[11] and on average one decay will result in the emission of 1 electron and 2.363 photons. The relation between the source activity, A, and the number of photons emitted per second, N_{photon}, is then calculated from:

$$N_{photon} = A \cdot (2.363 \pm 0.3\%) \quad [\text{photons s}^{-1}] \,, \tag{7}$$

where the uncertainty is estimated from an earlier version of the ^{192}Ir spectrum published by Duchemin and Coursol, 1984.[12] Fig. 2 shows the β spectrum for the ^{192}Ir nuclide and is calculated for the three major (95.35%) β^- transitions contributing to the spectrum. The last few percent of the β transitions are particles with energy less than 82 keV. A program written by L. van der Zwan, NRC, based on the work by W. G. Cross *et al.*[13] is used for the calculation, which includes corrections for both the influence of the Coulomb force field and the screening effect.

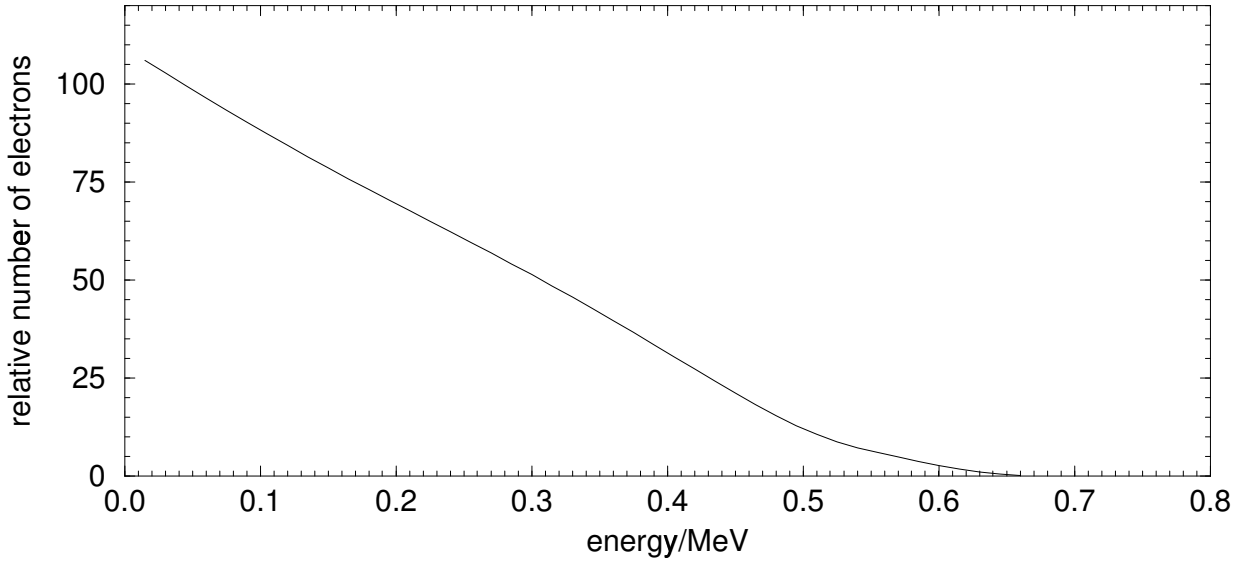

Figure 2: The β spectrum for ^{192}Ir radionuclide used as input spectrum for the Monte Carlo calculations. The spectrum is calculated using the data given by Duchemin and Coursol[11] for the three major (95.35%) β^- transitions contributing to the spectrum.

2. Monte Carlo calculations

2.1. Monte Carlo models of ^{192}Ir sources

Four types of ^{192}Ir sources are modelled - the seed sources manufactured by Best Industries, Inc., and by Alpha-Omega Services, Inc., the microSelectron-HDR source (manufactured by Nucletron International) and the VariSource (Manufactured by Varian Associates, Inc.). An older type of the microSelectron-HDR source is also modelled to be able to compare the calculated air-kerma strength per unit source activity to values reported by various authors. This source with a design nearly identical to the source used by the Gamma Med 12I afterloader has a 3.5 mm long and 0.6 mm diameter core of pure Ir encapsulated in stainless steel.[3,14]

The microSelectron-HDR source is assumed to consist of a 3.6 mm long cylinder with diameter 0.65 mm of pure Ir metal with the radioactive ^{192}Ir uniformly distributed in it. Around this core is a capsule with outer diameter of 0.9 mm made of AISI 316L steel, and connected to a 2.0 mm long steel cable with diameter 0.7 mm. Fig. 3 shows the geometry of the real microSelectron-HDR ^{192}Ir source (a), and the model used in the Monte Carlo calculations (b). The model consisting of cylindrical geometries is an approximation to the real geometry, since the user-code FLURZ calculates fluence for cylindrical geometries only.

The seed source from Best Industries, Inc., is 3.0 mm long, the diameter of the core is

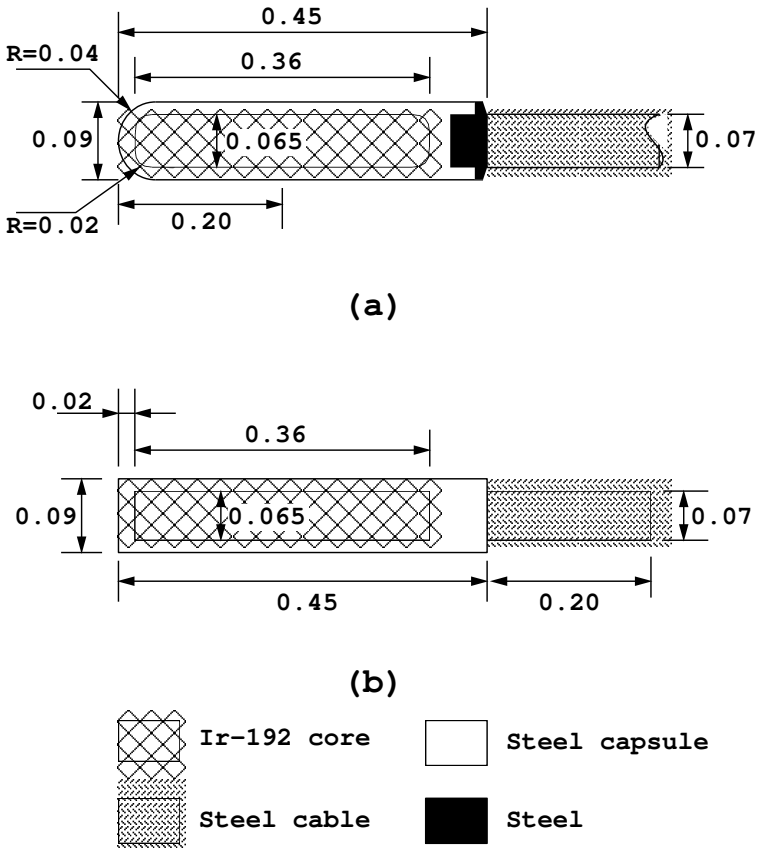

Figure 3: The microSelectron-HDR ^{192}Ir source. a) shows the geometry of the real source, while b) is the model used in the Monte Carlo calculations. Dimensions are given in cm.

0.1 mm, and the cladding is 0.2 mm thick consisting of stainless steel.[5] This core is 30% Ir and 70% Pt. The seed source from Alpha-Omega Services, Inc., is also 3.0 mm long, the diameter of the core is 0.30 mm and the cladding is 0.10 mm thick consisting of 99.9% Pt.[5] The core is 10% Ir and 90% Pt. In Fig. 4, the geometry of the two seed sources is shown.

All types of stainless steel in the sources were approximated by the composition of AISI 304 steel.[14] The composition, density, and effective atomic number, Z, of all materials used in the different types of sources are given in Table 1.

The core of the VariSource is 10.0 mm long with a diameter of 0.34mm[‡]. The encapsulation is Nitinol (manufactured by Memry Corporation). The diameter of the encapsulation is 0.6 mm and the ends are covered by 0.1 mm Nitinol and 2.5 m Nitinol (wire), respectively. In the model the 2.5 m Nitinol is reduced to 1.9 cm.

The scoring regions for the fluence in the transverse axis direction are 0.01 cm thick air cylinders for the surface and the 1 cm distance and 0.05 cm thick air cylinders for the greater distances. The length of the scoring region is 0.02 cm centered at the middle of the active length. No attenuation in these regions is assumed for the energies in these calculations ($>$ 1 keV).

[‡]Private communication with Stavros Prionas, Varian Associates, Inc.

Table 1: The materials used in the Monte Carlo calculations and their composition, density and effective atomic number. The air is dry air near sea level (1 atm.) and 20 °C.[15]

Material	Element	Composition [% by weight]	Density [g cm^{-3}]	Z_{eff}
Air (dry)			1.205E-03	8
	C	0.0124		
	N	75.5267		
	O	23.1781		
	Ar	1.2827		
Ir			22.39	77
Pt			21.41	78
Ir 10%, Pt 90%			21.508	78
	Ir	10		
	Pt	90		
Ir 30%, Pt 70%			21.704	78
	Ir	30		
	Pt	70		
Steel			8.02	26
(AISI 304)	Si	1		
	Cr	19		
	Mn	2		
	Fe	68		
	Ni	10		
Nitinol			6.42	26
	Ni	55.8		
	Ti	44.2		

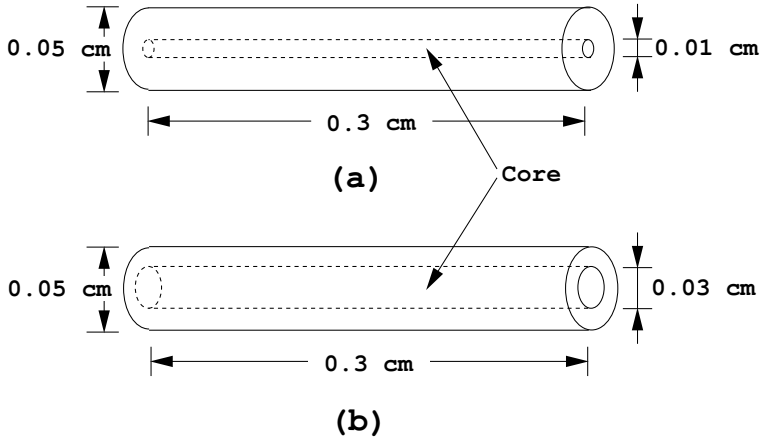

Figure 4: Model of seed sources from a) Best Industries, Inc., with a 30% Ir / 70% Pt core (stainless steel encapsulation), and b) Alpha-Omega Services, Inc., with a 10% Ir / 90% Pt core (platinum encapsulation).

In the calculations K-shell x-ray fluorescence and Rayleigh scattering are taken into account in all regions. The energy cut-off for electron transport is 2.0 MeV, which means that all energy transferred to electrons will be deposited at the point of the interaction and there is then no electromagnetic radiation loss. Photons are followed till they reach the cut-off energy of 0.001 MeV.

The total air-kerma is related to the photon fluence by

$$K_{air} = 1.602 \cdot 10^{-10} \int_{E_{min}}^{E_{max}} \varphi(E) \cdot E \cdot \left(\frac{\mu_{en}(E)}{\rho} \right) \cdot dE \quad \text{[Gy]} \ , \tag{8}$$

where $\varphi(E)$ [MeV^{-1} cm^{-2}] is the photon fluence per unit energy at energy E [MeV], and $\frac{\mu_{en}(E)}{\rho}$ [cm^2 g^{-1}] is the mass energy-absorption coefficient at energy E. The factor $1.602 \cdot 10^{-10}$ is required to convert K_{air} from MeV g^{-1} into Gy.

At the source surface, and at 1, 2, 5, 10, 20, and 50 cm distance from the center of the core at the transverse axis, the air kerma per initial particle is calculated from the fluence in 5 keV bins per source particle and the mass energy-absorption coefficients for dry air in the middle of each bin. The x-ray mass energy-absorption coefficients, $\frac{\mu_{en}}{\rho}$, for dry air are taken from the latest NIST compilation and shown in Fig. 5.[16]

When the user-code FLURZ is used, it calculates $\varphi'(E)$, the differential fluence spectrum in some volume per initial photon in the simulation. The program KERMADP[17] is used to calculate K'_{air}, the air kerma per initial photon in that same volume, using the following discrete equation:

$$K'_{air} = 1.602 \cdot 10^{-10} \sum_{E_{min}}^{E_{max}} \varphi'(E_i) \cdot E_i \cdot \left(\frac{\mu_{en}(E_i)}{\rho} \right) \cdot \Delta E \quad \text{[Gy photon}^{-1}\text{]} \ , \tag{9}$$

where E_i is the mid-point of each energy bin and ΔE is the bin size. The air-kerma rate,

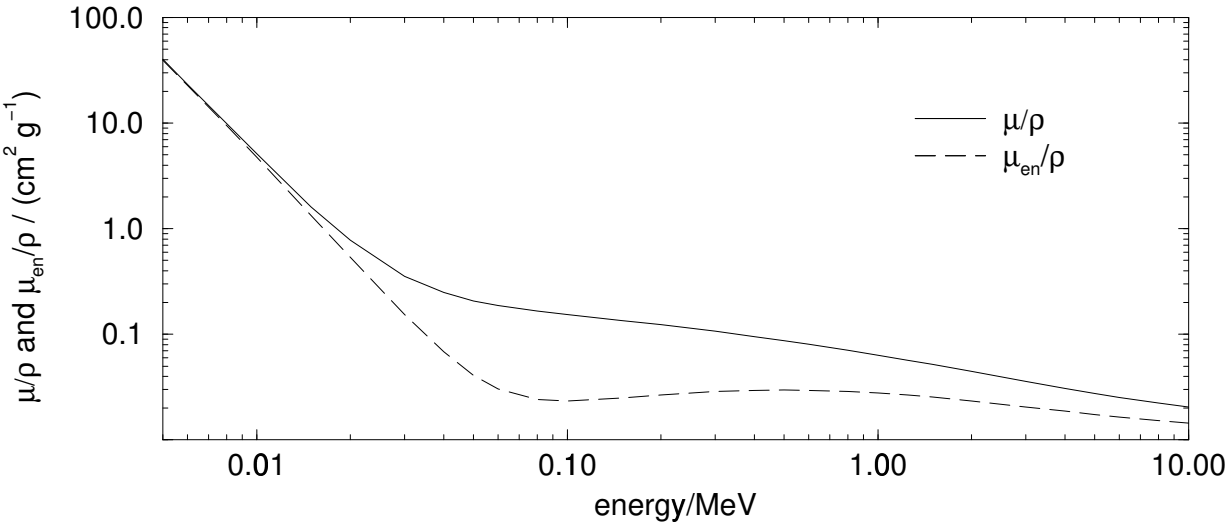

Figure 5: X-ray mass attenuation coefficients and mass energy-absorption coefficients for dry air (near sea level). From J. H. Hubbell and S. M. Seltzer, Report NISTIR 5632.[16]

$\dot{K}_{air}$, in [Gy s^{-1}] for a ^{192}Ir source of activity A in [Bq] is determined from:

$$\dot{K}_{air} = K'_{air} \cdot N_{photon} = 2.363 \cdot K'_{air} \cdot A \quad [\text{Gy s}^{-1}] \,, \tag{10}$$

where N_{photon} is given by Eq. 7. The air-kerma strength per unit source activity is then calculated using Eq. 1 divided by the activity:

$$S_k/A = \dot{K}_{air}(d) \cdot d^2/A = 2.363 \cdot K'_{air}(d) \cdot d^2 \quad [\text{Gy m}^2\ \text{s}^{-1}\ \text{Bq}^{-1}] \tag{11}$$

or in [U Bq^{-1}]

$$S_k/A = 3.6 \cdot 10^9 \cdot (2.363 \pm 0.3\%) \cdot K'_{air}(d) \cdot d^2 \quad [\text{U Bq}^{-1}] \tag{12}$$

2.2. Binning artefacts

Choosing the proper bin size in the Monte Carlo calculations is important, since 88% of the photon energies for the primary spectrum are in the upper half of 10 keV bins when divided into bins $0-10$ keV, $10-20$ keV, ..., $890-900$ keV.

The kerma is calculated using the mass energy-absorption coefficient at the middle of the energy bins. This may cause a binning artefact due to the large variation of the mass energy-absorption coefficient within the bin, especially for energies below 100 keV (see Fig. 5). The binning artefact was studied for the stainless steel encapsulated seed source for bin sizes of 10, 5 and 2 keV. Scoring in 5 keV bins instead of 10 keV bins increases the air-kerma rate by 0.6%, and scoring in 2 keV bins instead of 5 keV bins resulted in an increase of 0.04%. However, the smaller the bin size the more memory is required. The bin size of 5 keV is chosen as a compromise between smallest binning artefact and an acceptable amount of memory. The photon fluence spectrum for bremsstrahlung was scored in 10 keV bins,

which will not result in a significant binning artefact, since the bremsstrahlung spectrum is continuous.

Photons with energy below 210 keV contribute 2% of the total air-kerma strength for the stainless steel encapsulated seed source. It is the photons with energy above 210 keV that cause the difference in air kerma for different bin sizes.

2.3. Uncertainties

The sources have an uncertainty on the geometry while manufactured, which has not been accounted for. The sources are assumed identical to the models shown in Fig. 3 and Fig. 4, and the activity is assumed evenly distributed within the core. According to Büermann *et al.*[3] both assumptions have an uncertainty of 0.5%. Furthermore, there is an uncertainty on the interaction coefficients used in the calculations. The mass energy-absorption coefficient, $\frac{\mu_{en}}{\rho}$, has an uncertainty estimated to be 1% for energies above 30 keV and $5-10$% below 30 keV.[18] A total uncertainty on the air-kerma strength per unit activity due to geometry, activity distribution and interaction coefficients amounts to approximately 1.4%. The uncertainty stated in Table 4 showing the results of air-kerma strength per unit activity, only describes the statistical uncertainty (1 standard deviation) obtained through the Monte Carlo calculation.

The core is assumed to consist of Ir and Pt as specified for each source type. There may exist impurities in the core material, *e.g.* ^{60}Co. However, in small amounts this will not be of significance until the ^{192}Ir with a half-life of 73.8 days has decayed to very low activity comparable to the activity of the ^{60}Co (half-life 5.26 years).

^{192}Ir is produced when stable ^{191}Ir absorbs a neutron. The abundance of ^{191}Ir is 37% and the rest of stable Ir isotopes are ^{193}Ir.[5] Other radioactive isotopes of Ir and Pt will also be produced when absorbing neutrons, but all these (99%) have half-lives less than 20 hours[19] and will have decayed to negligible activity (1%) after a relatively short time (less than 6 days). The initial spectra for ^{192}Ir used in the calculations reported here may be considered very much like the actual spectrum from the isotopes within the source, when the sources are actually used.

3. Results

The Monte Carlo calculated photon spectra around the four types of encapsulated ^{192}Ir brachytherapy sources are given and the air-kerma strengths per unit source activity are estimated based on these spectra. The contribution to the air-kerma strengths from scattered photons and from bremsstrahlung are quantified and the influences of air filtration for both the encapsulated sources as well as the bare source are calculated. Finally, the contribution to the air-kerma strength from low-energy photons is estimated.

3.1. Photon fluence

The core and the encapsulating material attenuate the photons from the ^{192}Ir nuclide resulting in a modified photon spectrum outside each type of source. The Monte Carlo calculated photon spectra outside the four types of sources are shown in Fig. 6. The spectra for the bare source and the encapsulated sources are given in Appendices A1 - A5. The relative fluences of the main peaks in these spectra and for the bare source are shown in Table 2 together with the total fluence at 5 cm distance. From this table is seen that for the microSelectron-HDR source, the VariSource and the seed source from Alpha-Omega Services, Inc., the total fluences are less and the low-energy lines relatively smaller than for the seed source from Best Industries, Inc. This is due to the greater attenuation and scattering in the relatively larger amount of high-Z core material for the microSelectron-HDR source, the VariSource and the seed source from Alpha-Omega compared to the seed source from Best Industries. Also the type of encapsulating material effects the photon fluence.

Table 2: Relative photon fluence at 5 cm distance for the major lines in the four sources: microSelectron (a), Best Industries (b), Alpha-Omega (c) and VariSource (d) and for the ^{192}Ir radionuclide. The last line gives the total fluence at a distance of 5 cm with vacuum outside the sources. The lower cut-off energy of the fluence spectra is 0 keV.

Energy [keV]	Φ/Φ_{total} (a) [%]	Φ/Φ_{total} (b) [%]	Φ/Φ_{total} (c) [%]	Φ/Φ_{total} (d) [%]	Φ/Φ_{total} input [%]
60 - 70	3.6	4.2	3.9	3.6	4.5
295 - 300	11.5	12.1	11.7	11.5	12.2
305 - 310	12.2	12.7	12.3	12.2	12.7
315 - 320	33.6	35.0	34.2	33.6	35.0
465 - 470	21.2	20.5	21.2	21.2	20.2
Φ_{total} [cm^{-2}]	$2.741 \cdot 10^{-3}$	$3.055 \cdot 10^{-3}$	$2.806 \cdot 10^{-3}$	$2.741 \cdot 10^{-3}$	$3.183 \cdot 10^{-3}$

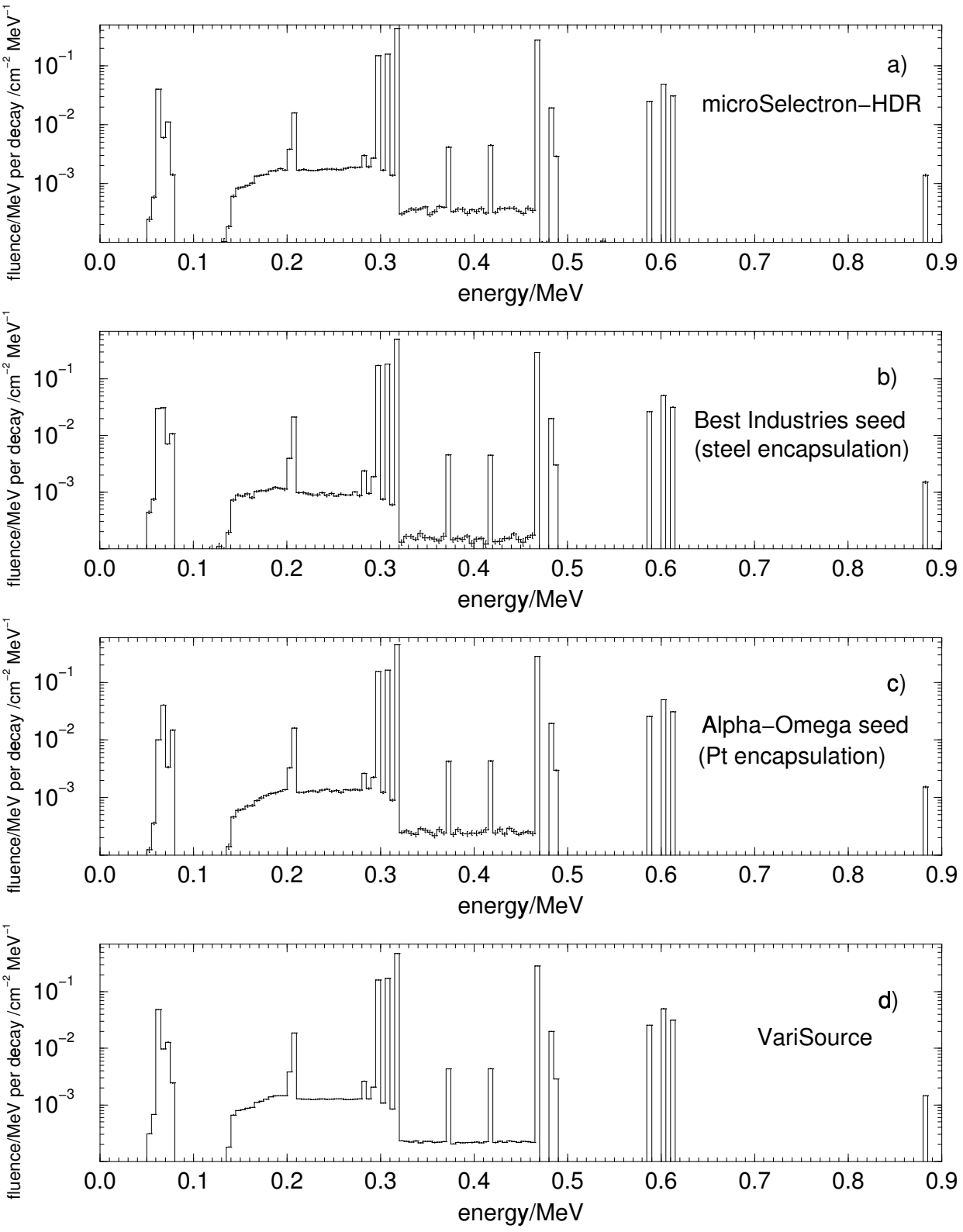

Figure 6: Fluence spectra in 5 keV bins for the microSelectron-HDR source (a), the stainless steel encapsulated seed source from Best Industries (b), the platinum encapsulated seed source from Alpha-Omega (c) and the VariSource (d) at 5 cm distance. No bremsstrahlung is included. Similar spectra are obtained at other distances when corrected for the inverse square law. Values are tabulated in Appendices A2 - A5.

3.2. Scatter-photon contribution

The ratio of scattered photons to total exiting photons for the seed sources agree completely with the amount reported by Thomason *et al.*,[2] *i.e.* $4-5\%$ of the photons exiting the stainless steel encapsulated seed source (Best Industries) and about 8% of those exiting the platinum encapsulated seed source (Alpha-Omega) are scattered. For the microSelectron-HDR source, also encapsulated in stainless steel, $9-10\%$ of the photons exiting are scattered, and for the Nitinol encapsulated VariSource the scattered photons amount to 7%. Both the amount of high-Z core material and the type of encapsulation effect the ratio of scattered photons. These scattered photons contribute $2-4\%$ of the total air-kerma strength depending on the source type. Table 4 shows that the core and encapsulation attenuate the air kerma from the bare-source photons by 12 to 23%, when the whole spectrum is taken into account.

3.3. Bremsstrahlung contribution

Bremsstrahlung photons are generated in the high atomic number Ir/Pt cores by the β^- decays, and they contribute to the air-kerma strength along with the photons originating from the primary photons. The β spectrum shown in Fig. 2 was used for the calculation of the bremsstrahlung contribution to the air-kerma strength for each of the four sources. The cut-off energy for electrons in these calculations was 10 keV (kinetic energy). For the microSelectron-HDR source, the VariSource and the platinum encapsulated seed source, bremsstrahlung increases the air-kerma strength by 0.2% and for the stainless steel source by 0.3%.

3.4. Air attenuation

Within the given uncertainties there is no difference between the results of calculations performed with air surrounding the source to calculations with vacuum around the source except for the bare source. The unfiltered spectrum from the bare source still includes photons of low energy (< 60 keV), which are attenuated in the air. For example 10 keV photons are attenuated 35% when passing through 50 cm of air, and for the bare source the air kerma for photons between 7 and 14 keV amounts to almost 10% of the total air kerma (see Fig. 8). The decrease in air-kerma rate for the bare source over the distance from 2 to 50 cm of air is only 3.4%.

3.5. Air-kerma strength per unit activity

The air-kerma strength per unit activity is estimated based on the Monte Carlo calculated fluence spectra around the four types of sources. In Table 3 the estimates are listed for different distances from each type of source and the statistical uncertainty is stated (1 standard deviation). These estimates do not include the bremsstrahlung contribution to the air-kerma strength, which increases the values by 0.2% for the microSelectron-HDR source, the VariSource and the platinum encapsulated seed source, and by 0.3% for the stainless steel encapsulated seed source.

Table 3: Estimates of S_k/A based on fluence spectra at different distances for the microSelectron-HDR source (new), the stainless steel encapsulated and the platinum encapsulated seed sources and the VariSource. The values do not include the bremsstrahlung contribution which increases the air-kerma strengths by $0.2 - 0.3\%$ (see Section 3.3.). The uncertainty is 1 standard deviation of statistical uncertainty.

Source type	microSelectron-HDR	Steel encapsulated seed	Pt encapsulated seed	VariSource
Distance [cm]	S_k/A [10^{-8} U Bq^{-1}]	S_k/A [10^{-8} U Bq^{-1}]	S_k/A [10^{-8} U Bq^{-1}]	S_k/A [10^{-8} U Bq^{-1}]
Surface	3.584 ± 0.001	2.8908 ± 0.0006	2.6493 ± 0.0005	0.769 ± 0.0001
1	9.626 ± 0.006	10.604 ± 0.005	9.829 ± 0.006	9.498 ± 0.002
2	9.700 ± 0.008	10.664 ± 0.008	9.888 ± 0.006	10.063 ± 0.002
5	9.711 ± 0.014	10.673 ± 0.014	9.892 ± 0.012	10.232 ± 0.004
10	9.709 ± 0.020	10.667 ± 0.018	9.891 ± 0.015	10.261 ± 0.006
20	9.726 ± 0.028	10.700 ± 0.024	9.935 ± 0.021	10.264 ± 0.007
50	9.710 ± 0.037	10.668 ± 0.033	9.889 ± 0.036	10.274 ± 0.012

On the source surface the air-kerma strength is lower than at distances from 1 cm and up. This is explained from the geometry of the source being a line and not a point. The geometry factor, $G(r,\theta)$, accounts for the variation of relative dose due only to the spatial distribution of activity within the source, ignoring photon absorption and scattering in the source.[5] For a line source the geometry factor is calculated from:

$$G(r,\theta) = \frac{\beta}{L \cdot r \cdot \sin\theta} \tag{13}$$

where L is the active length of the source, r is the distance to the point of interest, $P(r,\theta)$, β is the angle, in radians, subtended by the active source with respect to the point P, i.e. $\beta = \theta_2 - \theta_1$, and θ_1, θ_2 and θ are shown on Fig. 7.

For the microSelectron-HDR source, the seed sources and the VariSource the geometry factors times r^2 at the source surfaces are 0.3838, 0.2755 (for both seeds) and 0.0924, respectively. At distances from 1 cm and up, this value is approximately 1.0 except for the VariSource for which the distance must be 5 cm to consider it a point source. The ratios of the air-kerma strength at the source surface to that at 1 cm distance for the four sources are 0.372, 0.273, 0.270 and 0.081, respectively. The difference from the theoretical value is the influence of absorption and scatter in the core and in the encapsulating material. Core length, h, only affects the dose rate on the transverse axis at radial distances $r < 4h$, whereas the core diameter, d, influences the air-kerma strength at all radial distances.[20]

In Table 4 the estimated values of air-kerma strengths per unit source activity are shown as an average of the values listed in Table 3 for distances ranging from 2 to 50 cm (for the VariSource from 5 to 50 cm). For comparison with other reported S_k/A values, the values for the old type of the microSelectron-HDR source are estimated based on Monte

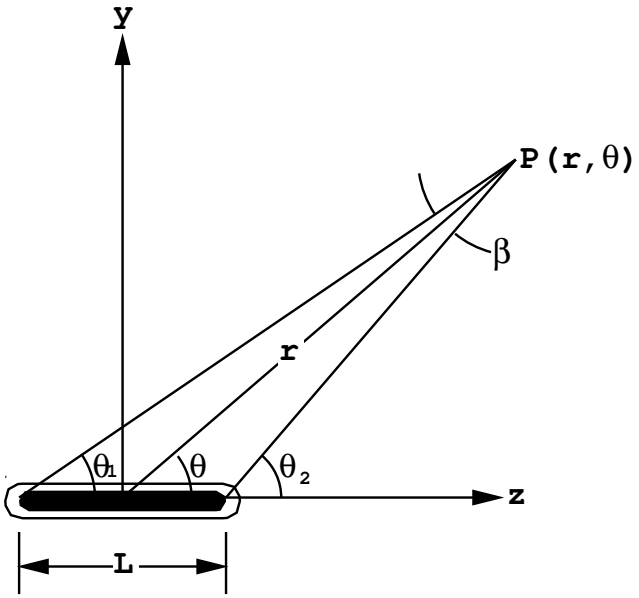

Figure 7: The parameters used for calculating the geometry factor, $G(r,\theta)$, for a line source. All angles are in radians.

Carlo calculation of photon fluence. The uncertainty is 1 standard deviation based on the 5 estimated S_k/A values for these distances not taking their uncertainties into account. At these distances the geometry factor is approximately 1. The values also include the bremsstrahlung contributions, which increases the S_k/A values for the microSelectron-HDR source, the VariSource and the platinum encapsulated seed source (Alpha-Omega) by 0.2% and the value for the stainless steel encapsulated seed source (Best Industries) by 0.3% compared to the value without bremsstrahlung. The results of earlier work on the same type of sources are shown as well (these do not include the bremsstrahlung contribution).

The air-kerma strengths per unit source activity for the old microSelectron-HDR source and for the bare source agree well with reported results from other authors. For the new microSelectron-HDR source the value is $0.6-0.7\%$ lower than for the old one. The core diameter of the old type was 0.6 cm (new 0.65 cm) and the stainless steel encapsulation 0.25 cm (new 0.1 cm) thick. For the seed sources there is a small difference in the air-kerma strengths calculated in this work and the results of Thomason's calculations.

Thomason used 10 keV bins for scoring, while the bin size was reduced to 5 keV in this work due to bin size artefacts. Our results suggest her values would be 0.6% higher using the smaller bins. In her calculations of exposure-rate constant, Λ_δ, the value was calculated for all photons exiting the source capsule with an energy greater than 11.3 keV (γ or x-rays of energy less than 11.3 keV are considered non-penetrating and are not included in Thomason's [1] and Glasgow *et al.*'s[8] values), and the bremsstrahlung was not taken into account. This work includes the contribution from bremsstrahlung, which is not included in the other reported values of S_k/A. For the bare source, the S_k/A values depend very much on the threshold energies. Büermann *et al.*[3] had a low-energy limit of 60 keV, and Glasgow and Thomason had a limit of 11.3 keV. The S_k/A value for $E > 11.3$ keV calculated in this work

Table 4: Air-kerma strength per unit source activity for different sources. The data are average values of the air-kerma strength per unit source activity based on fluence spectra at distances ranging from 2 to 50 cm (5 to 50 cm for the VariSource), and they are calculated for lower cut-off energies of the fluence spectra of 0, 11.3 and 60 keV for comparison with other reported values. The air-kerma strengths calculated in this work include the contribution from bremsstrahlung, which increases the S_k/A values without bremsstrahlung by 0.2% for the microSelectron-HDR source, the VariSource and the seed source from Alpha-Omega and by 0.3% for the seed source from Best Industries. The values in ( ) are calculated by us using the spectra given in the given reference and the mass energy-absorption coefficients from Hubbell and Seltzer.[16] The value of the total exposure-rate constant calculated by Glasgow *et al.* is corrected by 33.97/33.7, since the energy required to produce an ion pair in dry air has been re-evaluated since 1979 and his value was for humid air. The uncertainty is 1 standard deviation of statistical uncertainty (note that some are given in absolute values and some in per cent) except for the values from Büermann *et al.*[3] which includes uncertainties due to the interaction coefficients used in the Monte Carlo calculations (1%), uncertainty on the source geometry (0.5%), and uncertainty on the distribution of the activity within the core (0.5%) (see Section 2.3.).

Source	This work S_k/A [10^{-8} U Bq^{-1}]	Glasgow *et al.*[8] S_k/A [10^{-8} U Bq^{-1}]	Thomason[1] S_k/A [10^{-8} U Bq^{-1}]	Büermann *et al.*[3] S_k/A [10^{-8} U Bq^{-1}]
microSelectron				
> 0 keV	9.73 ± 0.01	-	-	-
> 11.3 keV	9.73 ± 0.01	-	-	-
> 60 keV	9.70 ± 0.01	-	-	-
old microSelectron				
> 0 keV	9.79 ± 0.02	-	-	-
> 11.3 keV	9.79 ± 0.02	-	-	-
> 60 keV	9.77 ± 0.02	-	-	$9.8 \pm 1.5\%$
VariSource				
> 0 keV	10.28 ± 0.02	-	-	-
> 11.3 keV	10.28 ± 0.02	-	-	-
> 60 keV	10.24 ± 0.02	-	-	-
Best Industries				
> 0 keV	10.71 ± 0.02	-	-	-
> 11.3 keV	10.70 ± 0.02	-	10.8 ± 0.1	-
> 60 keV	10.68 ± 0.02	-	-	-
Alpha-Omega				
> 0 keV	9.92 ± 0.02	-	-	-
> 11.3 keV	9.92 ± 0.02	-	9.95 ± 0.14	-
> 60 keV	9.92 ± 0.02	-	-	-
Bare source				
> 0 keV	11.95	-	(20.7)	-
> 11.3 keV	11.23	11.20 (11.23)	11.23 (11.15)	-
> 60 keV	10.88	(10.92)	(11.15)	$11.0 \pm 1\%$

is based on the assumption that the number of L-shell x-rays in the interval from 7.82 to 13.82 keV are evenly distributed. These x-rays are from the decay of the ^{192}Ir nuclide and they are removed from the filtered spectra due to attenuation in core and encapsulating material. Differences in spectral data results in the air-kerma strength per unit source activity being different by up to 0.7%. Also the small differences in the mass energy-absorption coefficients results in the values being different by up to 0.7%. However, in spite of the differences in spectra and mass energy-absorption coefficients, the value of the air-kerma strength per unit source activity for the bare source with a threshold energy of 11.3 keV varies by only 0.3%, *i.e.* the differences in spectra and $\frac{\mu_{en}}{\rho}$ values nearly cancel each other.

The uncertainty in the results from Büermann *et al.*[3] includes the uncertainties due to the interaction coefficients used in the Monte Carlo calculations (1%), uncertainty on the source geometry (0.5%), and uncertainty on the distribution of the activity within the core (0.5%). The total uncertainty is stated to be 1.5%. The low uncertainty on the other values only reflects the statistical uncertainty from the Monte Carlo calculation.

In Fig. 8 - 12 the accumulated air kerma is shown together with the relative number of photons given at a linear scale. The accumulated air kerma is the ratio of the air kerma below the energy given on the x-axis to the total air kerma for the spectra presented at 5 cm from the center of the source.

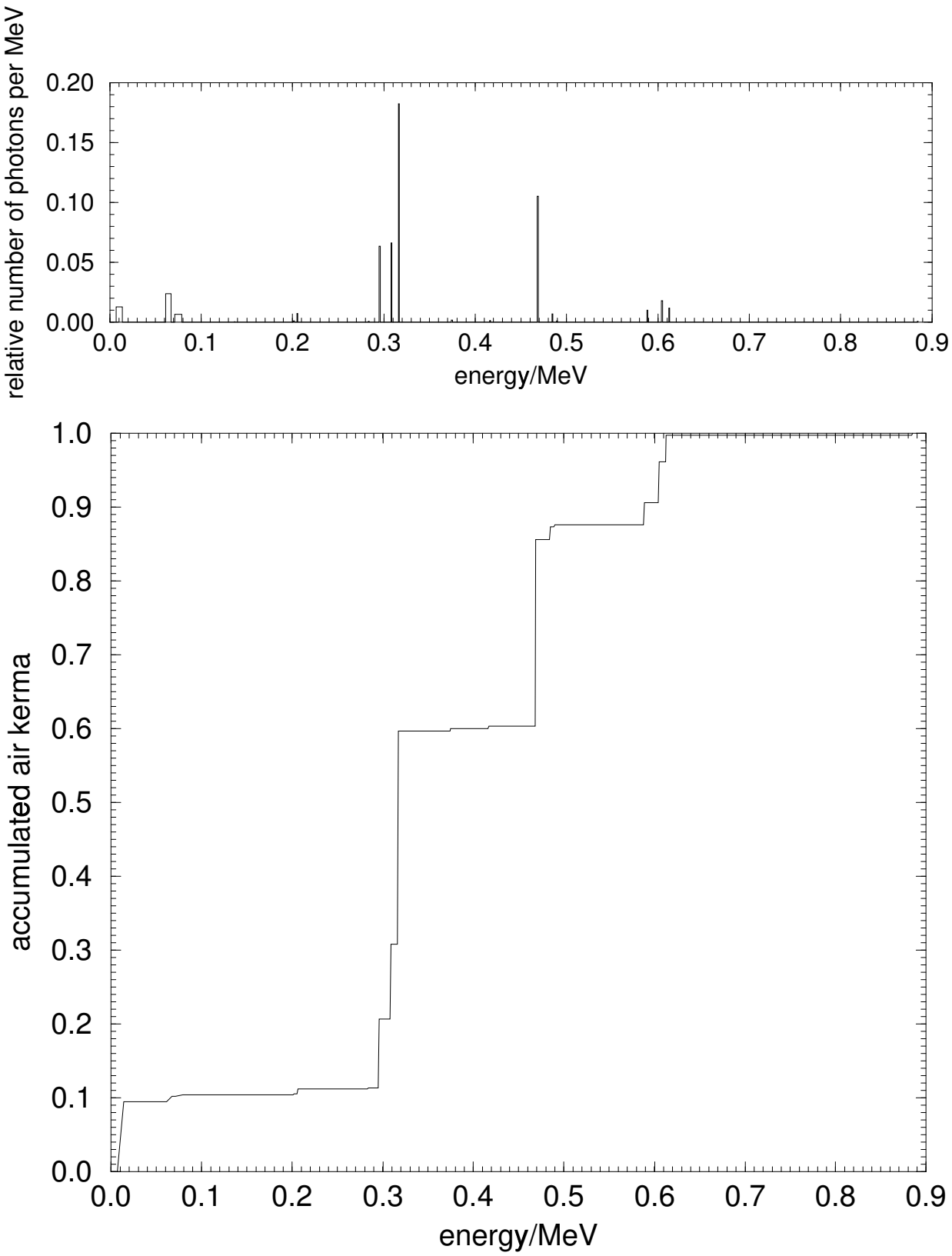

Figure 8: Accumulated air kerma for the ^{192}Ir radionuclide. The fluence spectrum for the source is shown at a linear scale above. Note the importance of photons from $7 - 14$ keV.

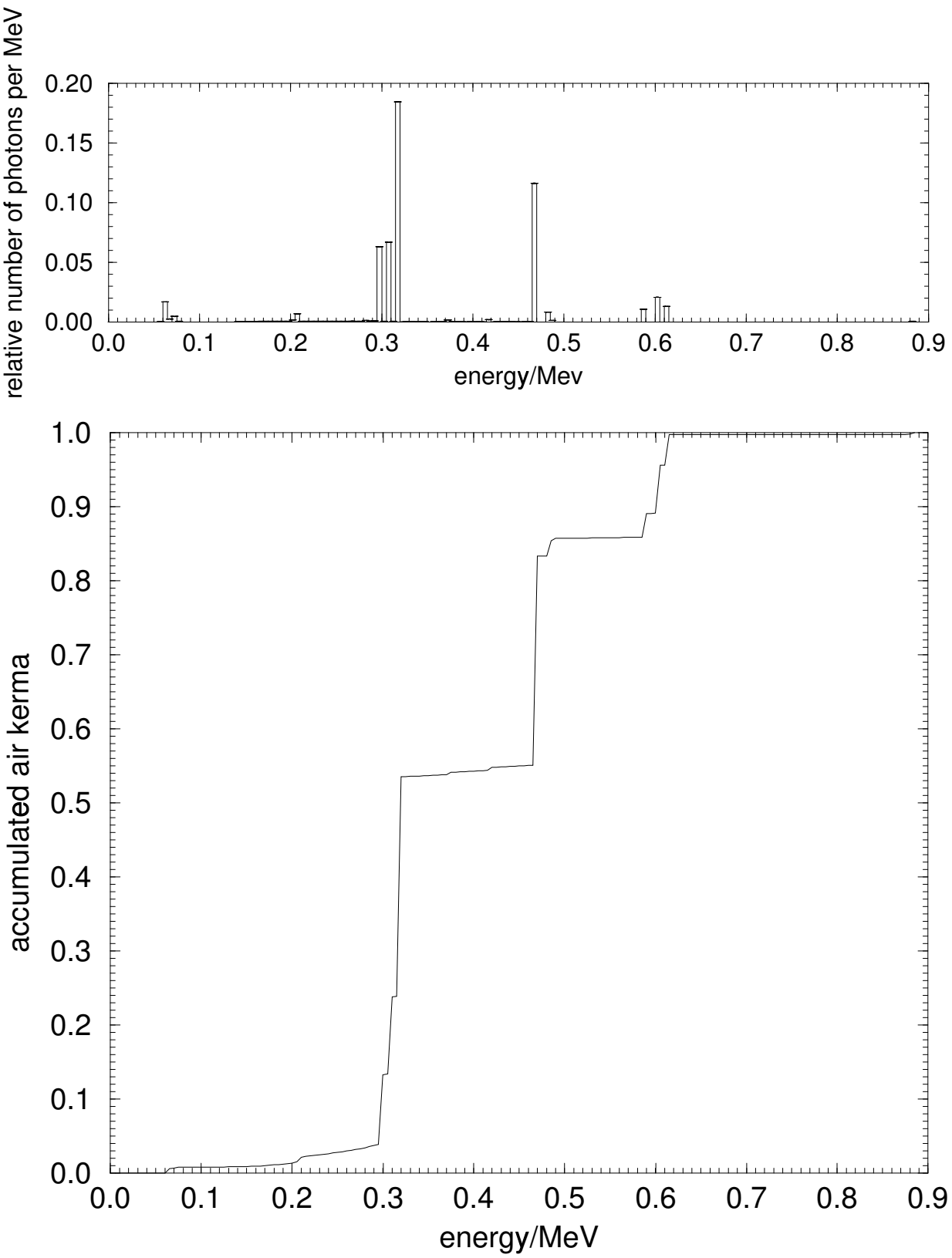

Figure 9: Accumulated air kerma for the microSelectron-HDR source. The fluence spectrum for the source is shown at a linear scale above.

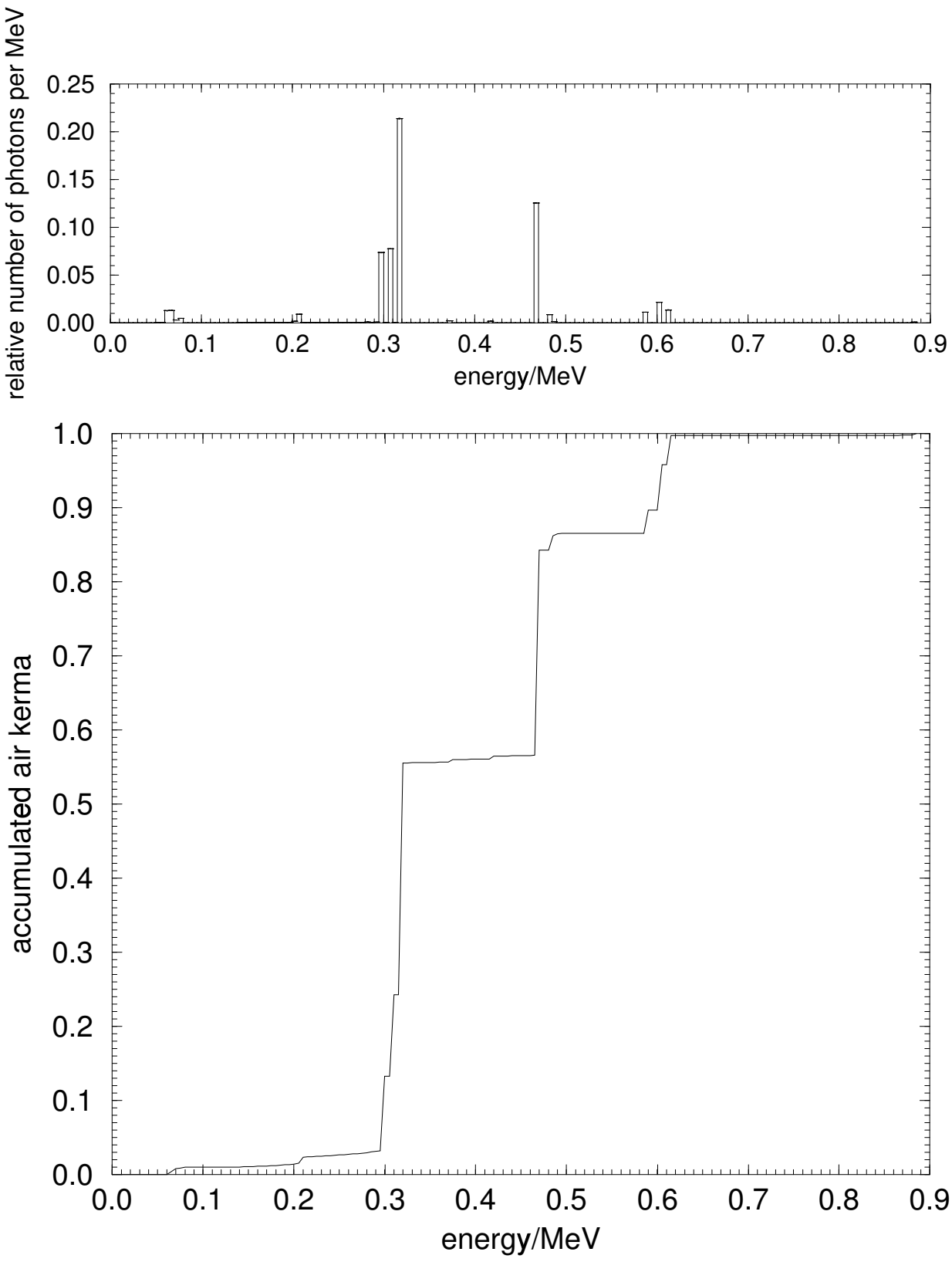

Figure 10: Accumulated air kerma for the seed source from Best Industries, Inc. The fluence spectrum for the source is shown at a linear scale above.

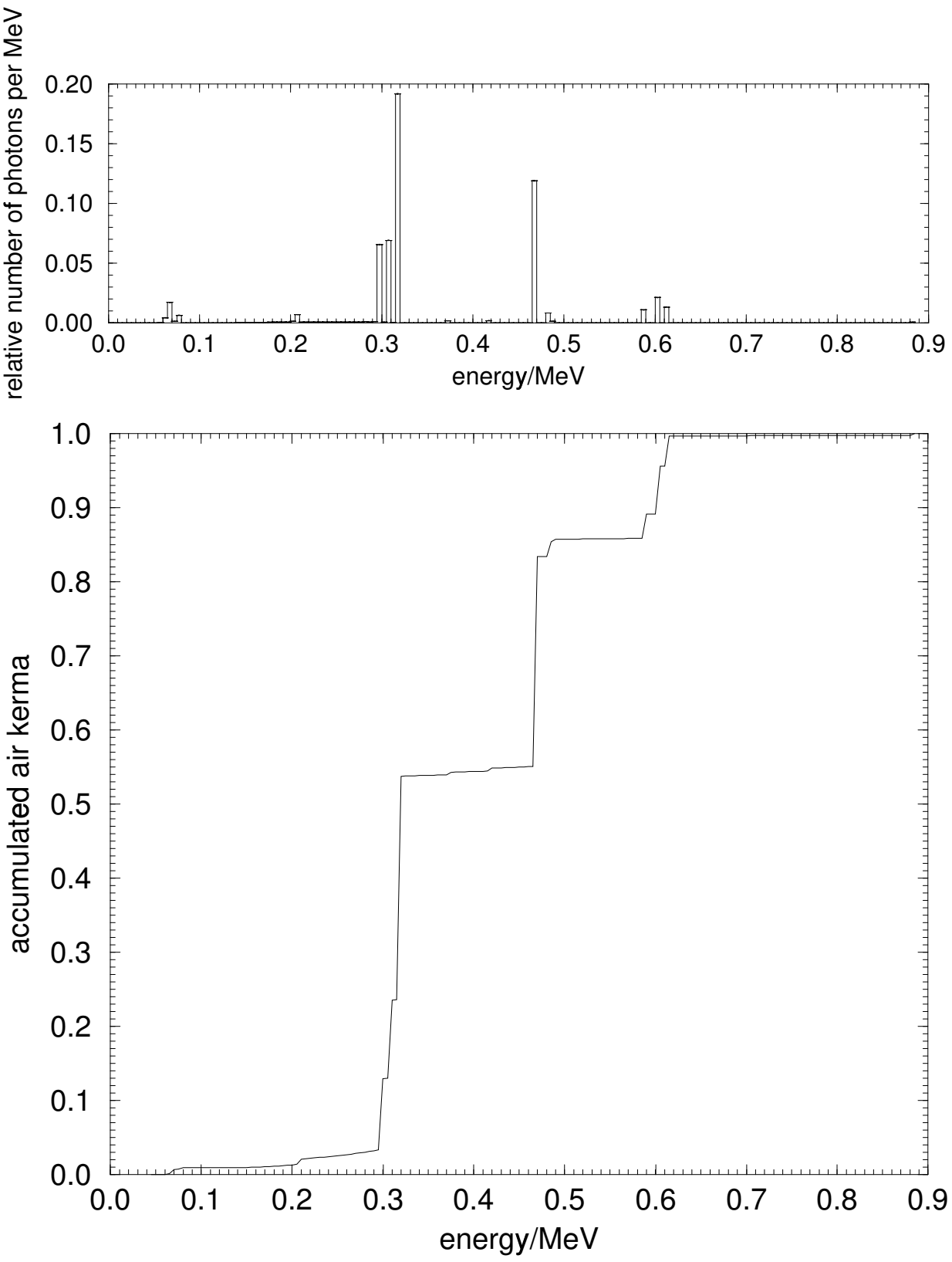

Figure 11: Accumulated air kerma for the seed source from Alpha-Omega Services, Inc. The fluence spectrum for the source is shown at a linear scale above.

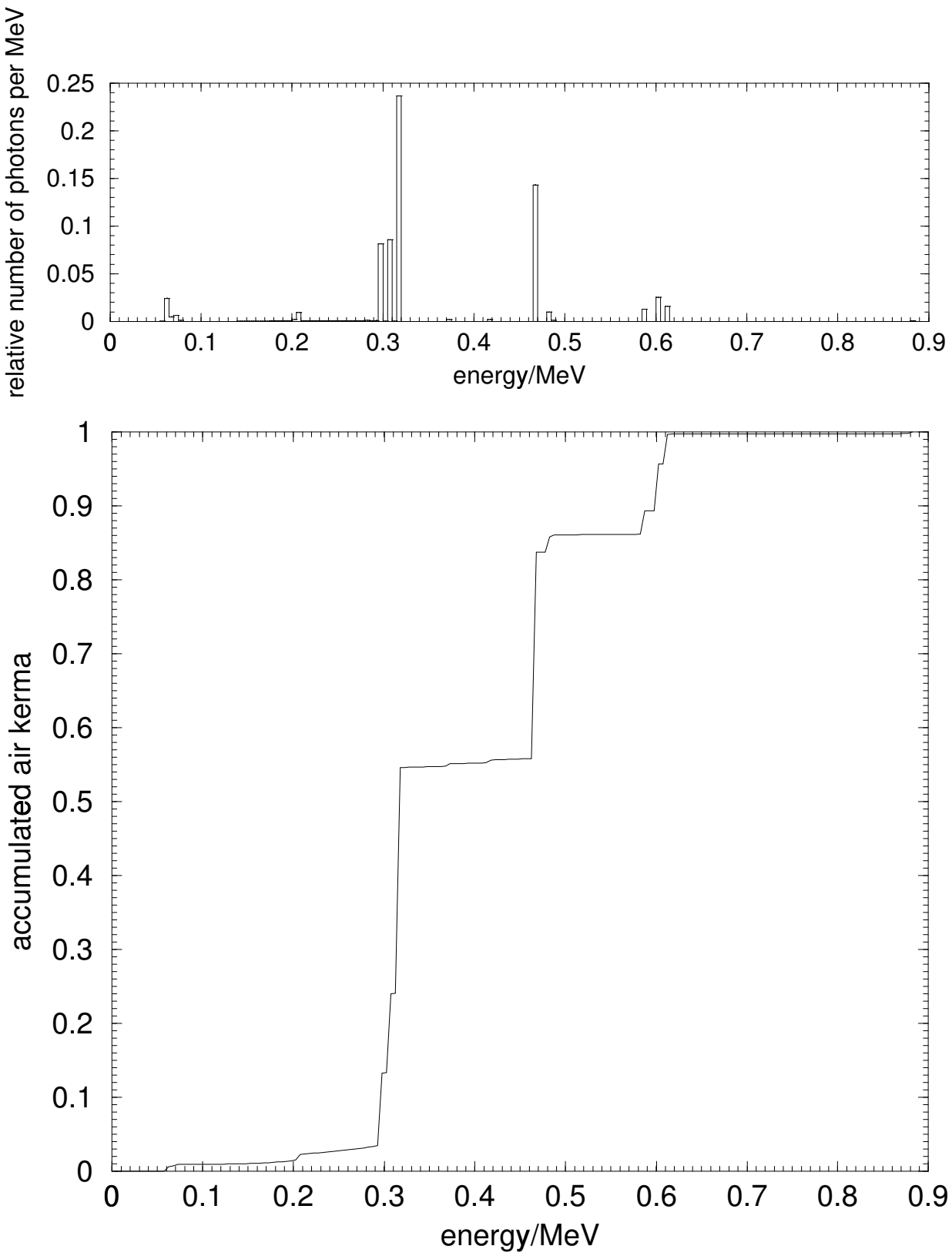

Figure 12: Accumulated air kerma for the VariSource. The fluence spectrum for the source is shown at a linear scale above.

3.6. Low-energy photons contribution to air kerma

The contribution of the low-energy photons to the air-kerma strength was studied for the encapsulated sources. Eliminating photons with energy less than 60 keV decreases the air-kerma strength by $0.2-0.3\%$, which is seen in Table 4. Eliminating the photons with energy less than 130 keV results in the air-kerma strength being reduced by 1% (Fig. 9 - 12).

The Monte Carlo calculation includes K-shell x-ray fluorescence but no L-shell x-rays. The energy of the K-shell x-rays is 76.1 and 78.4 keV for Ir and Pt, respectively, and 7.11 keV for stainless steel (Fe). A calculation with no x-ray fluorescence shows that the contribution to air-kerma strength from K-shell x-rays is about 0.2% for the microSelectron-HDR source. In Ir and Pt the L-shell x-rays have energies below 13.4 keV and 13.9 keV, respectively, and for the stainless steel the energy is below 0.85 keV. For stainless steel the L fluorescence yield is practically 0, and because of the low energy of the photons they will be absorbed within 1 cm of air and not show up in a measurement of air kerma. For L-shell x-rays from Ir and Pt no photons created in the core will pass through the encapsulation of the sources, and those created in the Pt encapsulation will have a high probability of undergoing photoelectric effect. The L-shell x-rays contribution to the air-kerma strength is thus likely negligible.

4. Summary and conclusions

The air-kerma strength per unit activity is calculated for the microSelectron-HDR source, the VariSource and stainless steel and platinum encapsulated seed sources at distances ranging from the surface of the source to 50 cm in both vacuum and air. The result for the microSelectron-HDR source (old type) is in agreement with the values from Büermann *et al.*[3] in 1994. The air-kerma strength per unit activity for the new type of microSelectron-HDR source is about $0.6 - 0.7\%$ lower compared to the old type. For the seed sources the air-kerma strengths per unit source activity are less than 1% smaller than the exposure-rate constants calculated by C. Thomason[1] in 1989. However, due to the bremsstrahlung contribution and the binning artefact, *i.e.* the difference between scoring in 10 keV bins instead of 5 keV bins, our values were expected to be about 1% higher than Thomason's values. The differences in data for the primary ^{192}Ir spectrum and mass energy-absorption coefficients for dry air explain this difference.

The effect of bin size for scoring the fluence was studied to reduce the binning artefact as well as using an adequate amount of memory. A bin size of 5 keV was found adequate.

The air-kerma strength for the bare source is $2 - 12\%$ higher than for the encapsulated sources due to the attenuation and absorption in the core and the encapsulating material. The bremsstrahlung contribution to the air-kerma strength is calculated for the four sources and increases air kerma strength by $0.2 - 0.3\%$. Scattered photons contribute $2 - 4\%$ of the total air-kerma strength.

The contribution of the low-energy photons to the air-kerma strength was studied for the encapsulated sources. Eliminating photons with energy less than 60 keV decreases the air-kerma strength by $0.2 - 0.3\%$ and eliminating the photons with energy less than 130 keV results in the air-kerma strength being reduced by 1%.

5. Acknowledgments

We wish to thank Carl Ross and Jan Seuntjens, Ionizing Radiation Standards, National Research Council of Canada, for valuable comments on this report. We also thank Stavros Prionas, Varian Associates, Inc., for information on the geometry of the VariSource.

A Appendix

A1 ^{192}Ir radionuclide

The photon spectrum for the ^{192}Ir radionuclide is given in Table 5. Photon emissions with absolute intensities less than 0.1% are omitted. The β spectrum for the ^{192}Ir radionuclide is given in Table 6. It is approximated by the β^- transitions for 95.35% of all β transitions. All spectral information is taken from Duchemin and Coursol, 1993.[11]

The spectra for the primary photons and electrons are placed in respectively
`$HENHOUSE/ensrc_spectra/Ir192_bare_1993.spectrum`
and
`$HENHOUSE/ensrc_spectra/Ir192_beta.spectrum`.

Table 5: Photon spectrum for the ^{192}Ir radionuclide. See also Fig. 1. There is no uncertainty associated with the values taken from Duchemin and Coursol.[11]

Energy interval or bin [keV]	Photons in bin per 100 decays [%]
7 - 14	5.8
61 - 67	10.72
71 - 79	2.892
136 -137	0.181
201 - 202	0.485
205 - 206	3.33
283 - 284	0.266
295 - 296	28.85
308 - 309	30.05
316 - 317	82.8
374 - 375	0.721
416 - 417	0.664
468 - 469	47.8
484 - 485	3.16
489 - 490	0.427
588 - 589	4.48
604 - 605	8.16
612 - 613	5.26
884 - 885	0.288
Total [photons/decay]	2.363

Table 6: β spectrum for the ^{192}Ir radionuclide. See also Fig. 2.

Top energy of bin [keV]	Relative number of emitted electrons
0.0225	53.99631
0.0375	52.15791
0.0525	50.3328
0.0675	48.52199
0.0825	46.72571
0.0975	44.94243
0.1125	43.16959
0.1275	39.64585
0.1575	37.89419
0.1725	36.1532
0.1875	34.42983
0.2025	32.73667
0.2175	31.0904
0.2325	29.51515
0.2475	28.04175
0.2625	26.7097
0.2775	25.50548
0.2925	24.29483
0.3075	23.06642
0.3225	21.81691
0.3375	20.54435
0.3525	19.24737
0.3675	17.92654
0.3825	16.58407
0.3975	15.22379
0.4125	13.85195
0.4275	11.11132
0.4575	9.768623
0.4725	8.467145
0.4875	7.228477
0.5025	6.078345
0.5175	5.046742
0.5325	4.168479
0.5475	3.482832
0.5625	2.902368
0.5775	2.343936
0.5925	1.816608
0.6075	1.330848
0.6225	0.898464
0.6375	0.533088
0.6525	0.249888
0.6675	0.065856

A2 microSelectron-HDR brachytherapy source

The intensity of the lines in the spectrum is shown in Table 7 and this spectrum is located at `$HENHOUSE/ensrc_spectra/Ir192_microSelectron.spectrum`.

Table 7: Photon spectrum 5 cm away on the transverse axis for the microSelectron source. The intensity is given as photon fluence (cm^{-2}) per MeV per 100 decays. The Compton scattered photons are averaged in the energy interval from 150 keV to 315 keV when no other peaks are present. The relative number of other scattered photons are insignificant and are not included. No bremsstrahlung is included since it will disappear in the uncertainty of the given photon spectrum. See Figure 6 a).

Energy interval or bin [keV]	Photon fluence (cm^{-2}) per MeV per 100 decays
60 - 65	3.991 ± 0.5%
65 - 70	0.601 ± 2.1%
70 - 75	1.107 ± 1.2%
75 - 80	0.140 ± 4.0%
150 - 200	0.165 ± 10%
200 - 205	0.382 ± 1.8%
205 - 210	1.587 ± 0.9%
210 - 280	0.165 ± 10%
280 - 285	0.298 ± 2.7%
285 - 290	0.165 ± 3.9%
290 - 295	0.271 ± 1.9%
295 - 300	14.835 ± 0.3%
300 - 305	0.165 ± 3.1%
305 - 310	15.757 ± 0.3%
310 - 315	0.165 ± 10%
315 - 320	43.509 ± 0.2%
370 - 375	0.415 ± 1.9%
415 - 420	0.448 ± 2.5%
465 - 470	27.416 ± 0.3%
480 - 485	1.926 ± 0.6%
485 - 490	0.289 ± 2.8%
585 - 590	2.493 ± 0.8%
600 - 605	4.888 ± 0.6%
610 - 615	3.074 ± 0.7%
880 - 885	0.138 ± 3.6%
Total [photon fluence/decay]	0.0064 ± 1.0%

A3 Stainless steel encapsulated seed source

The intensity of the lines in the spectrum is shown in Table 8 and this spectrum is located at `$HENHOUSE/ensrc_spectra/Ir192_best_industries.spectrum`.

Table 8: Photon spectrum 5 cm away on the transverse axis for the stainless steel encapsulated seed source from Best Industries. The intensity is given as photon fluence (cm^{-2}) per MeV per 100 decays. The Compton scattered photons are averaged in the energy interval from 140 keV to 305 keV when no other peaks are present. The relative number of other scattered photons are insignificant and are not included. No bremsstrahlung is included since it will disappear in the uncertainty of the given photon spectrum. See Figure 6 b).

Energy interval or bin [keV]	Photon fluence (cm^{-2}) per MeV per 100 decays
60 - 65	2.997 ± 0.5%
65 - 70	3.085 ± 0.6%
70 - 75	0.705 ± 1.3%
75 - 80	1.078 ± 1.5%
140 - 200	0.0944 ± 10%
200 - 205	0.396 ± 2.0%
205 - 210	2.126 ± 0.4%
210 - 280	0.0944 ± 10%
280 - 285	0.237 ± 3.4%
285 - 290	0.0994 ± 3.0%
290 - 295	0.187 ± 2.2%
295 - 300	17.369 ± 0.4%
300 - 305	0.0994 ± 3.2%
305 - 310	18.299 ± 0.3%
315 - 320	50.388 ± 10%
370 - 375	0.455 ± 1.6%
415 - 420	0.451 ± 1.8%
465 - 470	29.542 ± 0.3%
480 - 485	1.998 ± 0.7%
485 - 490	0.302 ± 2.0%
585 - 590	2.642 ± 0.7%
600 - 605	5.107 ± 0.6%
610 - 615	3.175 ± 1.0%
880 - 885	0.150 ± 4.2%
Total [photon fluence/decay]	0.0072 ± 1.0%

A4 Platinum encapsulated seed source

The intensity of the lines in the spectrum is shown in Table 9 and this spectrum is located at `$HENHOUSE/ensrc_spectra/Ir192_alpha_omega.spectrum`.

Table 9: Photon spectrum 5 cm away on the transverse axis for the platinum encapsulated seed source from Alpha-Omega Services, Inc. The intensity is given as photon fluence (cm^{-2}) per MeV per 100 decays. The Compton scattered photons are averaged in the energy interval from 160 keV to 305 keV when no other peaks are present. The relative number of other scattered photons are insignificant and are not included. No bremsstrahlung is included since it will disappear in the uncertainty of the given photon spectrum. See Figure 6 c).

Energy interval or bin [keV]	Photon fluence (cm^{-2}) per MeV per 100 decays
60 - 65	0.998 ± 1.2%
65 - 70	4.035 ± 0.5%
70 - 75	0.337 ± 2.7%
75 - 80	1.482 ± 0.9%
160 - 200	0.118 ± 10%
200 - 205	0.329 ± 2.0%
205 - 210	1.616 ± 0.7%
210 - 280	0.118 ± 10%
280 - 285	0.262 ± 1.9%
285 - 290	0.118 ± 3.3%
290 - 295	0.224 ± 3.0%
295 - 300	15.431 ± 0.3%
300 - 305	0.118 ± 5.0%
305 - 310	16.259 ± 0.3%
315 - 320	45.203 ± 0.2%
370 - 375	0.425 ± 2.1%
415 - 420	0.430 ± 2.2%
465 - 470	28.091 ± 0.2%
480 - 485	1.941 ± 1.1%
485 - 490	0.296 ± 2.2%
585 - 590	2.572 ± 0.8%
600 - 605	5.007 ± 0.4%
610 - 615	3.098 ± 0.5%
880 - 885	0.152 ± 2.8%
Total [photon fluence/decay]	0.0066 ± 1.0%

A5 VariSource

The intensity of the lines in the spectrum is shown in Table 10 and this spectrum is located at `$HENHOUSE/ensrc_spectra/Ir192_VariSource.spectrum`.

Table 10: Photon spectrum 5 cm away on the transverse axis for the VariSource. The intensity is given as photon fluence (cm^{-2}) per MeV per 100 decays. The Compton scattered photons are averaged in the energy interval from 150 keV to 315 keV when no other peaks are present. The relative number of other scattered photons are insignificant and are not included. No bremsstrahlung is included since it will disappear in the uncertainty of the given photon spectrum. See Figure 6 d).

Energy interval or bin [keV]	Photon fluence (cm^{-2}) per MeV per 100 decays
60 - 65	4.852 ± 0.2%
65 - 70	0.978 ± 0.4%
70 - 75	1.287 ± 0.3%
75 - 80	0.244 ± 0.7%
150 - 200	0.13 ± 10%
200 - 205	0.381 ± 0.6%
205 - 210	1.874 ± 0.4%
210 - 280	0.13 ± 10%
280 - 285	0.263 ± 0.8%
285 - 290	0.130 ± 1.1%
290 - 295	0.205 ± 0.8%
295 - 300	16.281 ± 0.1%
300 - 305	0.130 ± 10%
305 - 310	17.160 ± 0.1%
310 - 315	0.13 ± 0.9%
315 - 320	47.317 ± 0.1%
370 - 375	0.436 ± 0.3%
415 - 420	0.437 ± 0.9%
465 - 470	28.637 ± 0.1%
480 - 485	1.997 ± 0.2%
485 - 490	0.289 ± 0.4%
585 - 590	2.583 ± 0.2%
600 - 605	5.037 ± 0.2%
610 - 615	3.167 ± 0.3%
880 - 885	0.146 ± 0.9%
Total [photon fluence/decay]	0.0069 ± 1.0%

References

[1] C. Thomason. Dosimetry of Iridium-192 and Cesium-137 seed sources. *PhD Thesis, University of Wisconsin, Madison*, 1989.

[2] C. Thomason, T. R. Mackie, and M. J. Lindstrom. Effect of source encapsulation on the energy spectra of ^{192}Ir and ^{137}Cs seed sources. *Phys. Med. Biol.*, 36:495 – 505, 1991.

[3] L. Büermann, H.-M. Kramer, H. Schrader, and H.-J. Selbach. Activity determination of ^{192}Ir solid sources by ionization chamber measurements using calculated corrections for self-absorption. *Nucl. Instr. Meth.*, A339:369 – 376, 1994.

[4] T. P. Loftus. Standardization of Iridium-192 Gamma-Ray Sources in Terms of Exposure. *J Res. of the NBS*, 85:19 – 25, 1980.

[5] R. Nath, L. L. Anderson, G. Luxton, K. A. Weaver, J. F. Williamson, and A. S. Meigooni. Dosimetry of interstitial brachytherapy sources: Recommendations of the AAPM Radiation Therapy Committee Task Group No. 43. *Med. Phys.*, 22:209 – 234, 1995.

[6] ICRU. Radiation quantities and units. ICRU Report 19, ICRU, Washington D.C., 1971.

[7] ICRU. Radiation Quantities and Units. ICRU Report 33, ICRU, Washington D.C., 1980.

[8] G. P. Glasgow and L. T. Dillman. Specific γ-ray constant and exposure rate constant of ^{192}Ir. *Med. Phys.*, 6:49 – 52, 1979.

[9] D. C. Kocher. Radioactive dacay data tables. *Report DOE/TIC-11026, Department of Energy, USA*, 1981.

[10] NCRP Report 58. A Handbook of Radioactivity Measurements Procedures. *NCRP Publications, 7910 Woodmont Avenue, Bethesda, MD. 20814 USA*, 1985.

[11] B. Duchemin and N. Coursol. Reevalution de l'^{192}Ir. *Technical Note LPRI/93/018, DAMRI, CEA, France*, 1993.

[12] B. Duchemin and N. Coursol. LARA-90. *LARA-LMRI-1990, DAMRI/LMRI, CEA, France*, 1990.

[13] W. G. Cross, H. Ing, and N. Freedman. A short atlas of beta-ray spectra. *Phys. Med. Biol.*, 28:1251 – 1260, 1983.

[14] J. F. Williamson and Z. Li. Monte Carlo aided dosimetry of the microselectron pulsed and high dose-rate ^{192}Ir sources. *Med. Phys.*, 22:809 – 819, 1995.

[15] F. H. Attix. *Introduction to Radiological Physics and Radiation Dosimetry.* Wiley, New York, 1986.

[16] J. H. Hubbell and S. M. Seltzer. Tables of X-ray mass Attenuation Coefficients and Mass Energy-Absorption Coefficients 1 keV to 20 MeV for Elements Z = 1 to 92 and 48 Additional substances of Dosimetric Interest. Technical Report NISTIR 5632, NIST, Gaithersburg, MD 20899, 1995.

[17] B. R. B. Walters, D. W. O. Rogers, and K. R. Shortt. Simulation of a Cesium Irradiator using the BEAM Monte Carlo Code. *NRC Report PIRS - work in progress*, 1998.

[18] J. H. Hubbell. Photon Cross Sections, Attenuation Coefficients, and Energy Absorption Coefficients From 10 keV to 100 GeV. *NBS Report NSRDS-NBS 29*, 1969.

[19] E. Browne and R. B. Firestone. *Table of Radioactive Isotopes, Ed V S Shirley.* (Wiley, New York), 1986.

[20] R. Wang and R. S. Sloboda. Influence of source geometry and materials on the transverse axis dosimetry of ^{192}Ir brachytherapy sources. *Phys. Med. Biol.*, 43:37 – 48, 1998.